Two-Dimensional Thermal Boundary Layer Corrections for Convective Heat Flux Gauges

M. Kandula[1]
Sierra Lobo, Inc., John F. Kennedy Space Center, Florida 32899, USA

G. Haddad[2]
NASA Kennedy Space Center, Florida 32899, USA

This work presents a CFD (Computational Fluid Dynamics) study of two-dimensional thermal boundary layer correction factors for convective heat flux gauges mounted in flat plate subjected to a surface temperature discontinuity with variable properties taken into account. A two-equation $k-\omega$ turbulence model is considered. Results are obtained for a wide range of Mach numbers (1 to 5), gauge radius ratio, and wall temperature discontinuity. Comparisons are made for correction factors with constant properties and variable properties. It is shown that the variable-property effects on the heat flux correction factors become significant

Nomenclature

c	=	sound speed
c_p	=	specific heat
h	=	heat transfer coefficient
k	=	thermal conductivity
L	=	reference plate length
M	=	Mach number
Pr	=	Prandtl number
q	=	heat flux
R	=	gas constant; also radius of gauge
Re	=	Reynolds number
r	=	recovery factor
St	=	Stanton number
T	=	temperature
u^*	=	friction velocity, $\sqrt{\tau_w/\rho}$
x	=	streamwise direction
y	=	lateral coordinate
z	=	coordinate normal to the wall
z^+	=	zu^*/ν
η	=	correction factor for h
ϕ	=	$(T_{w1}-T_{w2})/(T_{w1}-T_{aw})$
γ	=	ratio of specific heats
ρ	=	density
μ	=	dynamic viscosity

[1] Sr. Principal Investigator, Associate Fellow AIAA.
[2] Sr. Engineer, Integration Branch, Launch Services Program, Member AIAA.

ν = kinematic viscosity, μ/ρ

τ_w = wall shear stress

ζ = $(T_{w2}-T_{w1})/(T_{w1}-T_{aw})$

Subscripts

1 = plate
2 = gauge
A = area-averaged
aw = adiabatic wall (recovery)
L = length-averaged
w = wall
∞ = free-stream

I. Introduction

Substantial errors are encountered in plug-type or Schmidt-Boelter–type metallic convective heat flux gauges when they are mounted in insulating structures typical of high-temperature applications involving aerodynamic heating (heat shield) and rocket engine exhaust gases (rocket nozzles). Because of surface temperature discontinuity (thermal mismatch between the gauge and the structure), the thermal boundary layer is altered, and the heat flux measured (sensed) by the gauge deviates considerably from the true heat flux that would be measured if the gauge material and the structure material were identical. Experiments (Reynolds et al.[1,2], Bachmann[3], Taylor et al.[4]) and analysis (Rubesin[5], Eckert[6]) suggest that a variable surface temperature distribution can produce a marked increase or decrease in the local and average convective heat transfer rates to a surface in both laminar and turbulent flow. For reviews on this subject, see Diller[7] and Neumann[8].

Correction factors have been proposed previously based on two-dimensional (2D) flat-plate boundary layer integral analysis with power law velocity and temperature profiles (e.g., Rubesin[5], Reynolds et al.[1], Westkaemper[9]). These analyses are based on constant thermal properties, and suffer from a number of simplifying assumptions. Two-dimensional CFD calculations at Mach 4 on a flat plate by Kandula and Reinarts[10] accounted for the effect of property variations on the correction factors.

Three-dimensional (3D) CFD computations (variable property) by Kandula et al.[11] for circular heat flux gauges indicate that 3D heat flux corrections generally exceed those given by 2D CFD solutions (variable property), especially for small gauges. It is shown later in the text that the differences between 2D and 3D CFD variable property solutions for the heat flux correction factors are smaller relative to the differences between the CFD

solutions (both 2D and 3D variable property) and the 2D constant property integral solution. This consideration suggests that 2D CFD variable property solutions serve as a useful guide for rapid estimates of heat flux corrections factors. Furthermore, the 3D CFD calculations for the estimation of corrections factors require a separate grid system for each value of gauge radius and thus entail additional grid generation and computational time. Also, the 3D CFD solutions presented in Ref.11 are primarily concerned with Mach 2 and Mach 4 only.

The purpose of this report is to extend the 2D CFD study of Kandula and Reinarts[10] to a wider range of Mach numbers (1 to 5), and to further illustrate the role of property variations. This article is based on Ref. 12.

II. Review of 2-D Integral Solutions for Constant Properties

A. Local heat transfer coefficient

Fig.1 displays the schematic of a heat flux gauge mounted flush on a flat plate (top view). The heat flux gauge is idealized to be 2D (with width $W - L$) even though in reality it has a circular cross section, which introduces 3D thermal boundary layer effects. Under these circumstances, we have the following thermal boundary conditions at the surface representing a temperature discontinuity:

$$\begin{aligned} T_w &= T_{w1} \qquad 0 < x < L \\ &= T_{w2} \qquad l \le X \le W \\ &= T_{w1} \qquad x > W \end{aligned} \tag{1a}$$

Consider now the flow past a 2D flat plate with a surface temperature discontinuity of the form

$$\begin{aligned} T_w &= T_{w1} \qquad 0 < x < L \\ &= T_{w2} \qquad x > L \end{aligned} \tag{1b}$$

The prescription of this boundary condition, instead of eq. (1a), is equivalent to ignoring the effect of the surface temperature discontinuity at the downstream end of the gauge ($x > W$) on the local heat transfer coefficient on the gauge. This assumption is justified because of the constant pressure boundary layer type flow considered here (as evidenced later in Fig. 5, displaying the local Stanton number with and without a surface temperature discontinuity).

This scheme thus requires only a single 2D solution that can furnish estimates necessary for the quasi-2D solution incorporating arbitrary gauge diameter $(W-L)$.

With the aid of an integral method with assumed power law profiles for velocity and temperature, Rubesin[5] and later Reynolds et al.[1,2] obtained an expression for the local heat transfer coefficient $h(x,L)$ in turbulent incompressible flow in the form

$$\frac{h(x,L)}{h(x,0)} = b + \zeta\left[1-\left(\frac{L}{x}\right)^{m_1}\right]^{m_2} \qquad x > L \tag{2}$$

where $b = (T_{w1} - T_{aw})/(T_{w2} - T_{aw})$, $\zeta = (T_{w2} - T_{w1})/(T_{w2} - T_{aw})$

Here, $h(x,0)$ denotes the local heat transfer coefficient on an isothermal plate with constant wall temperature T_{w1}. The exponents m_1 and m_2 are 39/40 and –7/39, respectively, from Rubesin[5], and 9/10 and –1/9 from Reynolds et al.[1,2], the latter valid over a wider range of Reynolds numbers. In (2), the heat transfer coefficient is defined as (Eckert[6], Kays and Crawford[13], Schlichting[14], White[15])

$$q = h(T_w - T_{aw}) \tag{3}$$

The corresponding local heat flux ratio is expressed by

$$\frac{q_2(x,L)}{q_1(x)} = 1 - \phi\left[1-(L/x)^{m_1}\right]^{m_2} \tag{4}$$

where $\phi = (T_{w2} - T_{w1})/(T_{w1} - T_{aw})$.

For very small values of L/x, $q_2/q_1 \to 1-\phi$, which depends on temperatures only, and independent of geometric parameters (Hornbaker and Rall[16]).

B. Length-averaged heat transfer coefficient

Based on the integral solution of Reynolds et al.[1,2], Westkaemper[9] derived a length-averaged heat transfer coefficient $\bar{h}_L$ over the heat flux gauge as

$$\eta_L = \frac{\bar{h}_L}{h\left(\frac{W+L}{2},0\right)} = bF(L/W) + \zeta H(L/W) \tag{5}$$

where $\bar{h}_L = \bar{h}(W,L)$ is given by

$$\bar{h}_L = \frac{Q}{(W-L)(T_{w2}-T_{aw})}, \quad Q = \int_L^W q(x)dx = \int_L^W h(x,L)(T_{w2}-T_{aw})dx \tag{6}$$

The factors F and H are defined by

$$F = c_k \frac{5}{4}\frac{\left|1-(L/W)^{4/5}\right|}{(1-(L/W))}, \quad H = c_k \frac{5}{4}\frac{(L/W)^{4/5}}{(1-L/W)}\left[(W/L)^{9/10}-1\right]^{3/9} - F(L/W) \tag{7}$$

where $c_k = 1$. Later, Knox[17] pointed out an error in Westkaemper's equations for F and H. Considering that

$$h\left(\frac{W+L}{2},0\right) \propto h(W,0)\left(\frac{2}{1+L/W}\right)^{1/5} \tag{8}$$

it was shown that the correction is provided by

$$c_k = \left[2/(1+L/W)\right]^{1/5} \tag{9}$$

III. 2-D CFD Analysis for Variable Properties

A. Grid and flow solution

Fig. 2 shows the grid (118×72) for a 2-D flat plate of length $2L$, subjected to a surface temperature discontinuity. The plate leading edge is maintained at $x/L = 0$. The boundary condition of wall temperature discontinuity is expressed by

$$\begin{aligned} T_w &= T_{w1} \qquad 0 < x/L < 1 \\ &= T_{w2} \qquad 1 < x/L < 2 \end{aligned} \tag{10}$$

Upstream of the plate leading edge, an inviscid plate length ($-0.5 < x/L < 0$) is also considered. A grid height of $z/L = 1$ is included. The grid is clustered both in the normal direction (near the wall) and in the axial direction (near the leading edge and near the surface temperature discontinuity). The first three cells near the wall in the normal direction have a uniform cell size $\Delta z/L = 10^{-5}$, with $z^+ < 0.3$ at the wall providing resolution of the viscous sublayer. Beyond the third cell, the grid is clustered with a stretching factor of 1.15.

Solution for the velocity and temperature distributions has been obtained by the OVERFLOW Navier-Stokes code[18,19]. A zonal two-equation $k-\omega$ Shear Stress Transport (SST) turbulence model due to Menter[20] has been utilized. Freestream boundary conditions are considered at $x/L = -0.5$ and $z/L = 1$. An extrapolation condition is considered at $x/L = 2$. The variation of viscosity and thermal conductivity with temperature is accounted for by Southerland's correlations[15]. A constant value of Pr=0.71 is assumed. Doubling the number of grid cells in the wall-normal direction has changed the local Stanton number less than one percent, thus ensuring grid independence of the solution.

With regard to the surface temperature discontinuity, a study by Nansteel et al.[21] has shown that the heat flux generally exhibits a *non-integrable singularity* at the temperature discontinuity, leading to an unbounded heat transfer (integrated heat flux), as the streamwise grid spacing at the discontinuity is indefinitely diminished. Under such circumstances, the numerical solution for heat transfer is dependent on the streamwise grid size in a logarithmic manner. For further details and methods of overcoming this difficulty, Ref. 21 may be consulted. By incorporating a small insulated region near the discontinuity (representing a more physically realistic circumstance

or smoothing), the singularity is shown to be avoided. However, in the present configuration, calculations ($M = 4, \mathrm{Re} = 10^6, T_{w1} = 778\,K, T_{w2} = 333\,K$) have shown that by decreasing the axial grid cell size by 50 percent, the heat flux correction factor has been increased only by about 0.6 percent (from 1.435 to 1.444). Thus it is believed that the problem of discontinuous singularity does not appreciably affect the present results.

B. Quasi–2-D extension

Kandula and Reinarts[10] considered a quasi–2-D extension to approximately account for the cylindrical geometry of the heat flux gauge (Figure 3). At any lateral plane of the gauge, the flow is assumed quasi–2-D so that an area-averaged heat flux correction factor $\bar{h}_A$ incorporating the 3-D effects can be estimated based on the 2-D results (both variable property CFD and constant property integral solutions) corresponding to the geometry and boundary conditions in Figure 2:

$$\bar{\eta}_A = \bar{h}_A / h\left(\frac{W+L}{2}, 0\right) \tag{11}$$

where $\bar{h}_A = \dfrac{2}{\pi r^2} \displaystyle\int_{y'=0}^{R} \bar{h}_L(W', L')(2x')dy', \quad x = R\cos\theta, \quad y = R\sin\theta.$

Calculations suggest that the quantities $\bar{h}_A$ and $\bar{h}_L$ denoting quasi–2-D and 2-D corrections do not appreciably differ from one another. For example, for $R/L = 0.01$, $M = 4, \mathrm{Re} = 10^6, T_{w1}/T_{aw} = 1.6$, the quantity $\bar{h}_A$ is only 2.5 percent higher than $\bar{h}_L$.

IV. Results and Comparison

Fig. 4a. displays the temperature contours near the surface temperature discontinuity, as obtained by the 2D CFD (variable property) solution for values of T_{w1} = 778 K (1400 R), T_{w2} = 333 K (600 R) and T_∞ = 288 K (518 R). The emergence of a new thermal boundary layer past the discontinuity is evident. The corresponding contours for the constant property solution are displayed in Fig. 4b.

The distribution of local Stanton number with and without the temperature discontinuity is sketched in Figure 5a. For validation purposes, the local Stanton number for the isothermal case (without the discontinuity) is compared with the recommended flat plate correlation for turbulent heat transfer from an isothermal flat plate (Reynolds et al.[1] as

$$St_x \, \mathrm{Pr}^{0.4} = 0.0296 \, \mathrm{Re}_x^{-0.2} \left(T_w / T_a\right)^{-0.4}$$

which is valid for air (Pr=0.7) and $10^6 < \mathrm{Re}_x < 10^7$. Satisfactory agreement is noted between the CFD result and the correlation. Because of the relatively low Reynolds number, the boundary layer is initially laminar, and transition to turbulence is occasioned shortly downstream of the leading edge (Kandula and Wilcox[22]). In the presence of a step-wall temperature jump, a sharp rise in local heat transfer coefficient is noted near the discontinuity, followed by a decreasing value with distance from the discontinuity as the newly formed thermal boundary layer thickens.

Fig. 5b presents a comparison of 2D CFD solutions for constant and variable properties with and without surface temperature discontinuity. The deviation between the constant property and variable property solutions may be explained by flow and thermal considerations as follows. The shear stress term $\frac{\partial}{\partial y}\left(\mu \frac{\partial u}{\partial y}\right)$ in the momentum equation, and the viscous dissipation term $\mu\left(\frac{\partial u}{\partial y}\right)^2$ and the heat conduction term $\frac{\partial}{\partial y}\left(k \frac{\partial T}{\partial y}\right)$ appearing in the energy equations are effected by the variation of properties μ and k with temperature within the boundary layer. Consequently, both q_2 and q_1 are expected to be affected by the variation of properties, the effect on the former being more prominent.

As indicated in section III, quasi-2D heat flux correction factors are obtained from 2D solutions approximately accounting for the circular geometry. All subsequent results presented here as 2D CFD and integral are actually quasi-2D results derived from the 2D solutions applied to the particular gauge size. The 3D CFD solution (Kandula et al.[11]) corresponds to a full three dimensional thermal boundary layer flow over the circular gauge mounted in a flat plate.

A comparison of the heat flux correction factors for $M = 4$ and $R/L = 0.01$ is provided in Figure 6a. Results for quasi–2-D CFD for both constat property (CP) and variable property (VP) and quasi–2D constant property integral results are compared. The absolute value of ratio q_2/q_1 increases with absolute value of ϕ. In many practical applications involving aerodynamic heating, we have plate wall temperatures below the recovery temperature, as heat is conducted into the plate material, so that only negative values of ϕ are pertinent. It is seen from the CFD results that the effect of variable properties in this range of ϕ is to lower the heat flux correction factors relative to those from constant properties. The results also suggest that the absolute values of q_2/q_1 from 2D CFD are significantly higher than those from constant-property integral correlations. Heat flux corrections for $M = 2$ are presented in Fig. 6b. The trends of the heat flux corrections factors are essentially similar tot hose shown for $M = 4$ (Fig. 6a).

Fig. 7 shows the variation of q_2/q_1 as a function of R/L as predicted by various theories. The predictions suggest that q_2/q_1 decreases with an increase in the value of R/L. In general, the CFD results accounting for constant properties exceed considerably the constant property integral solutions. On the other hand, a direct comparison of the CFD results suggest that the variable property CFD solutions provide q_2/q_1 that are lower than those from constant property solutions. To validate the theory, experimental data[23] for $M = 4$ and $\mathrm{Re} = 10^6$ from ground tests at NASA Marshall Hot Gas Test Facility (HGF), employing hydrogen-air combustion are also shown. The heat flux data were obtained from Schmidt-Boelter gauges (4.76 mm diameter, aluminium). For a brief description of the test facility, see Ref. 11. The plate-gauge system is operated in dynamic (transient) mode. The data at 10.2 atm stagnation pressure (p_0) corresponds to $T_{w1}/T_{aw} = 0.508$ and $T_{w2}/T_{aw} = 0.303$ and those at 13.93 atm correspond to $T_{w1}/Taw = 0.515$ and $T_{w2}/T_{aw} = 0.296$. Comparison of the theory with the data suggests that the test data corresponding to $R/L = 0.01$ and $R/L = 0.025$ are seen to lie between the 2D and the 3D CFD variable property solutions. These comparisons thus tend to highlight the importance of the 3-D boundary layer effects and of variable property effects.

A direct comparison between 2-D CFD results at M=1, 2, 3, 4 and 5 is displayed in Figure 8, showing the effect of Mach number on the heat flux correction factors. The results reveal that at a given value of ϕ (ϕ is negative here) the correction factor increases as the Mach number increases, as is to be expected owing to the role of compressibility and property variations. However, if the parameter T_{w2}/T_{aw} is held constant, the various lines should come closer.

V. Conclusions

Comparison of 2-D correction factors for convective heat flux gauges submitted to a surface temperature discontinuity as obtained from CFD indicate that the effect of property variations is significant. It is also shown that the constant property integral solutions are inadequate for predicting heat flux corrections, especially for small gauges.

Acknowledgments

This work has been supported by the Launch Services Program at the NASA Kennedy Space center. Discussions with Professor R.-H. Chen of the University of Central Florida are appreciated. The authors would like to thank the reviewers fro valuable suggestions and criticism that considerably improved the manuscript.

References

[1]Reynolds, W.C., et al., "Heat transfer in the turbulent incompressible boundary layer II– Step-wall temperature distribution," NASA Memo 12-2-58W, December 1958.

[2]Reynolds, W.C., et al., "A summary of experiments on turbulent heat transfer from a nonisothermal flat plate,"*Journal of Heat Transfer*, Vol. 82, 1960, pp. 341-348.

[3]Bachmann, R.C., et al., "Investigation of heat-flux measurements with calorimeters," ISA Trans., Vol. 4, 1965, pp. 143-151.

[4]Taylor, R.P., et al., Heat transfer measurements in incompressible turbulent boundary layer with step wall temperature boundary conditions, *Journal of Heat Transfer*, Vol. 112, 1990, pp. 245-247.

[5]Rubesin, M.W., The effects of an arbitrary surface temperature variation along a flat plate on the convective heat transfer, NACA TN 2345, April 1951.

[6]Eckert, E.R.G., and Drake, R.M., Analysis *of Heat and Mass Transfer*, 2nd ed., McGraw-Hill, New York, 1972.

[7]Diller, T.E., "Advances in heat flux measurements," in: J.P. Hartnett, T.F. Irvine (Eds.), Advances in Heat Transfer, Academic Press Inc., New York, Vol. 23, 1993, pp. 279-368.

[8]Neumann, R.D., "Thermal instrumentation – A state-of-the-art review," WL-TR-96-2107, Wright-Patterson Air Force Base, Ohio, 1996.

[9]Westkaemper, J.C., "On the error in plug-type calorimeters caused by surface temperature mismatch," *Journal of Aerospace Sciences*, Vol. 28, 1961, pp. 907-908.

[10]Kandula, M., and Reinarts, T., "Corrections for convective heat flux gauges subjected to a surface temperature discontinuity," AIAA-2002-3087, 2002.

[11]Kandula, M., Haddad, G.F., and Chen, R.-H., "Three dimensional thermal boundary layer corrections for circular heat flux gauges mounted in a flat plate with a surface temperature discontinuity," *International Journal of Heat and Mass Transfer*, Vol. 50 , 2007, pp.713-722.

12 Haddad, G.F., Kandula, M., and Chen, R.-H., "Two-dimensional correction factors for convective heat flux gauges installed in a flat plate with a surface temperature discontinuity," *13th International Heat Transfer conference*, Sydney, August 2006.

[13]Kays, W.M., and Crawford, M.E., *Convective Heat and Mass Transfer*, 2nd ed., McGraw-Hill, New York, 1980.

[14]Schlichting, H., *Boundary Layer Theory*, 7th ed., McGraw-Hill, New York. 1979.

[15]White, F.M., *Viscous Fluid Flow*, 2nd ed., McGraw-Hill, New York, 1991.

[16]Hornbaker, D.R., and Rall, D.L., "Thermal perturbations caused by heat-flux transducers and their effect on the accuracy of heating rate measurements," *ISA Transactions*, Vol. 3, 1964, pp.123-130.

[17]Knox, E.C., "A critique on correlating heat transfer results for temperature mismatch," Remtech Report RTN 158-02, March 1987.

[18]Jespersen, D.C., et al., "Recent enhancements to OVERFLOW," AIAA-97-0644, January 1997.

[19]Kandula, M., and Buning, P.G., "Implementation of LU-SGS algorithm and Roe upwinding scheme in OVERFLOW thin-layer Navier-Stokes code," AIAA-94-2357, 1994.

[20]Menter, F.R., Two-equation eddy viscosity turbulence model for engineering applications, AIAA Journal, Vol. 32, 1994, pp. 1598-1605.

[21]Nansteel, M.W., Sadhal, S.S., and Ayyaswamy, P.S., "Discontinuous boundary temperatures in heat transfer theory," in: Significant Questions in Buoyancy Affected Enclosure on Cavity Flows, ed. J.A.C. Humphrey, C.T. Avedisian, B.W. Le Tourneau, and M.M. Chen, ASME HTD-Vol. 60, pp. 123-126, 19xx.

[22]Kandula, M., and Wilcox, D.C., "An examination of $k-\omega$ turbulence model for boundary layers, free shear layers and separated flows," AIAA-95-2317, 1995.

[23]Strobel, F., Grudgen, J., Reinarts, T., and Rusell, G., "The use of heat flux gauges for hot wall TPS applications," *Space Technology and Applications International Forum (STAIF)*, February 2005.

Captions to Figures

Fig. 1 Circular heat flux gauge mounted in a flat plate with a discontinuity in wall temperature.

Fig. 2 Schematic of the grid for flow over a 2D flat plate.

Fig. 3 Quasi–2D representation of flow over the heat flux gauge.

Fig. 4 Temperature contours in the vicinity of the wall temperature discontinuity, as obtained from 2D CFD solution.

Fig. 5a Distribution of local Stanton number along a flat plate with a wall temperature discontinuity, as obtained from 2D CFD solution (variable property).

Fig. 5b Comparison of local Stanton number along a flat plate from 2D CFD constant property and variable property solutions.

Fig. 6a Comparison of heat flux correction factors for M=4 and R/L=0.01.

Fig. 6b Comparison of heat flux correction factors for M=2 and R/L=0.01.

Fig. 7 Comparison of heat flux correction factor for M=4 and R/L=0.01.

Fig. 8 Variation of heat flux correction factors with Mach number for R/L = 0.01 from 2D CFD with variable properties.

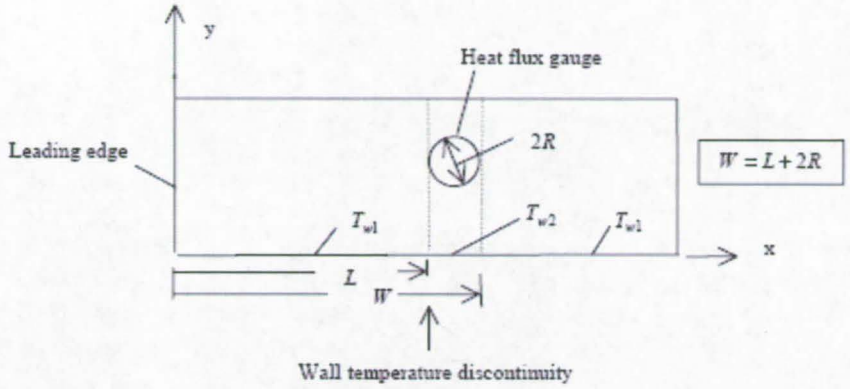

Fig. 1 Circular heat flux gauge mounted in a flat plate with a discontinuity in wall temperature.

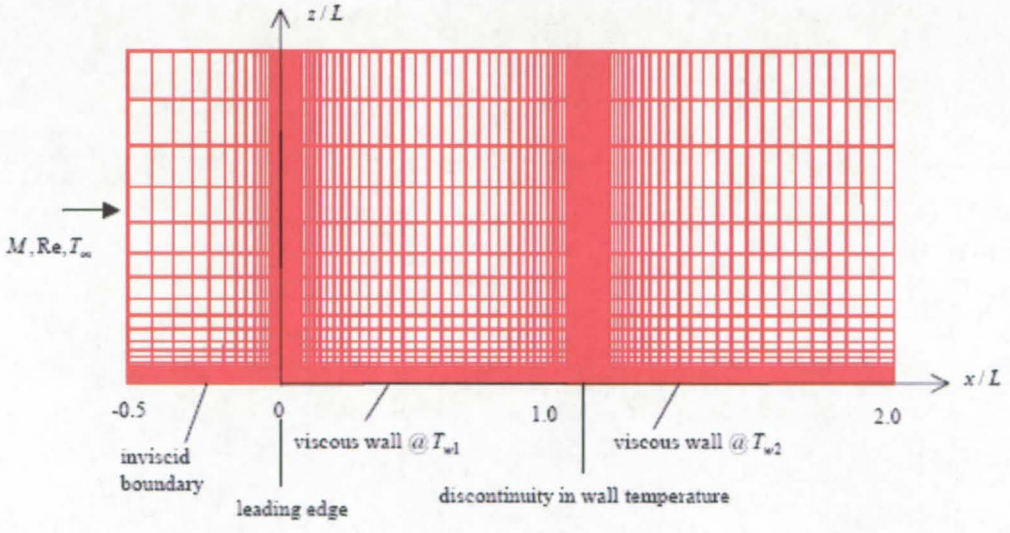

Fig. 2 Schematic of the grid for flow over a 2D flat plate.

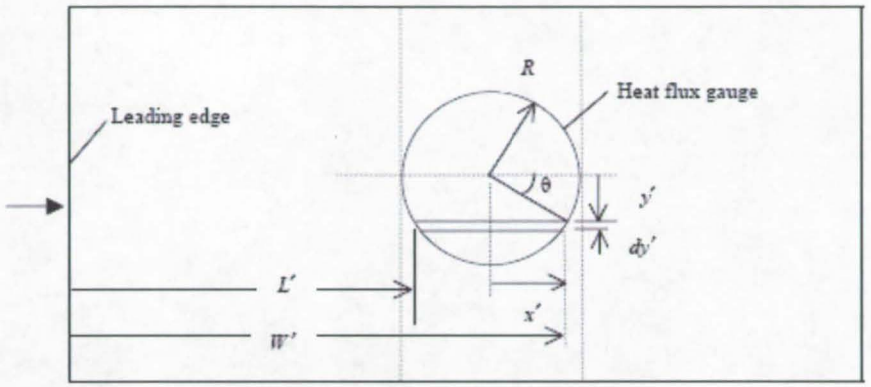

Fig. 3 Quasi–2D representation of flow over the heat flux gauge.

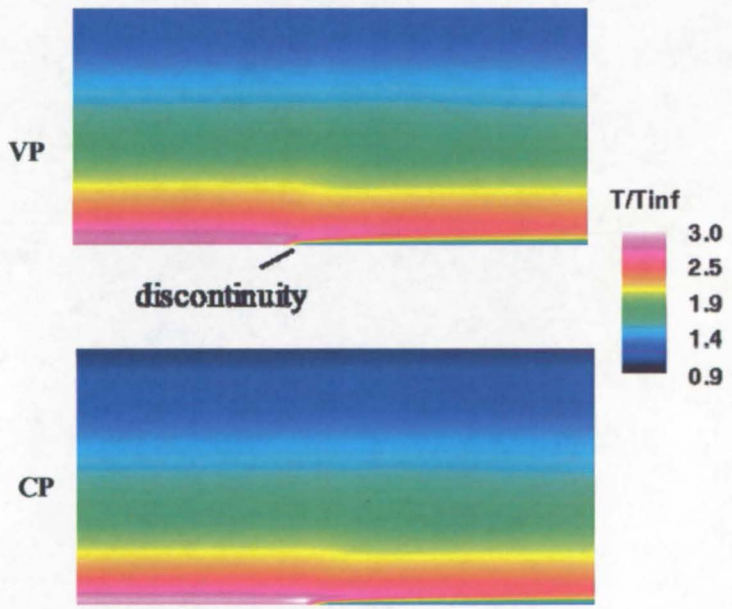

Fig. 4 Temperature contours in the vicinity of the wall temperature discontinuity, as obtained from 2D CFD solution.

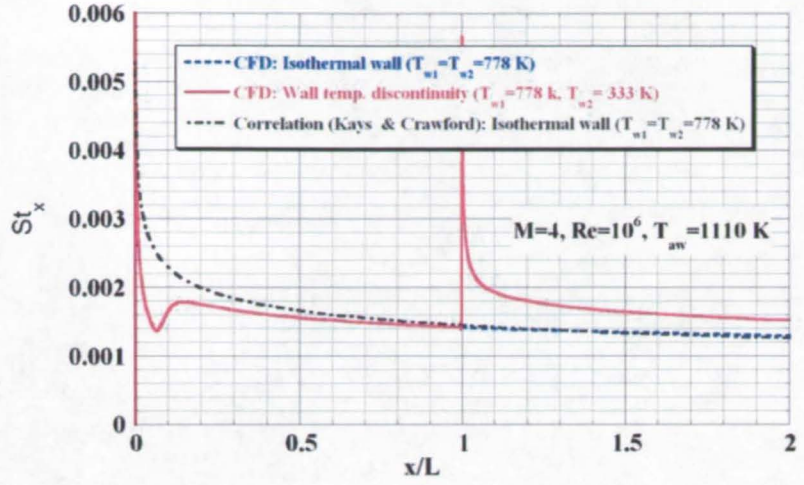

Fig. 5a Distribution of local Stanton number along a flat plate with a wall temperature discontinuity, as obtained from 2D CFD solution (variable property).

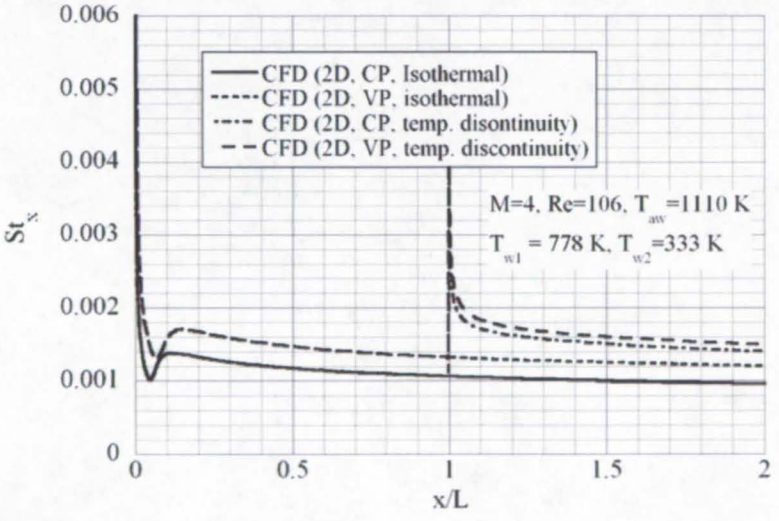

Fig. 5b Comparison of local Stanton number along a flat plate from 2D CFD constant property and variable property solutions.

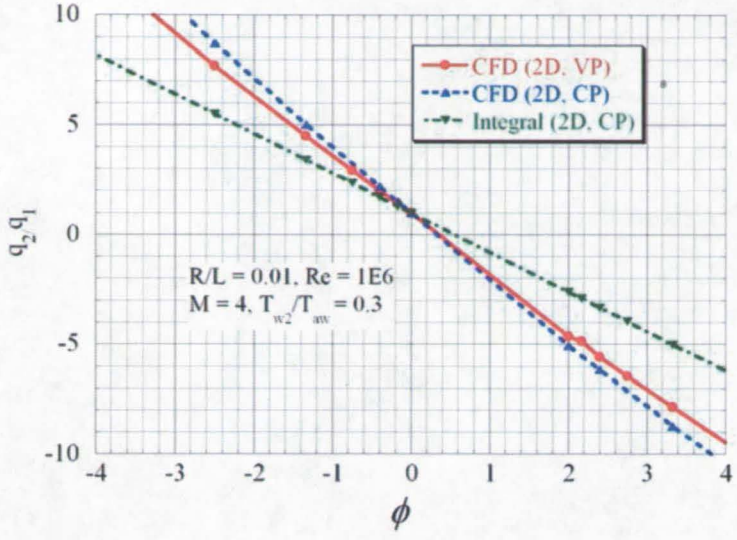

Fig. 6a Comparison of heat flux correction factors for M=4 and R/L=0.01.

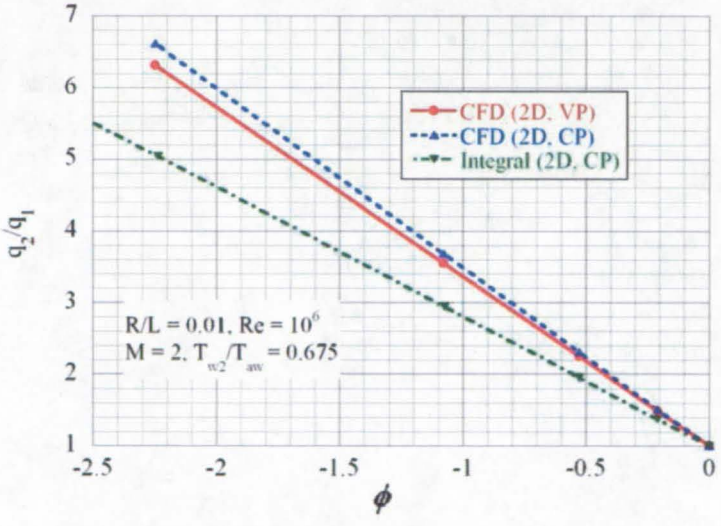

Fig. 6b Comparison of heat flux correction factors for M=2 and R/L=0.01.

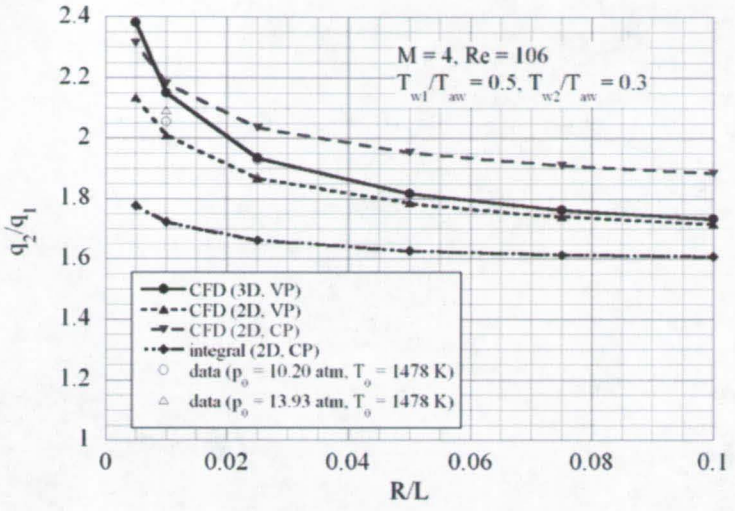

Fig. 7 Comparison of heat flux correction factor for M=4 and R/L=0.01.

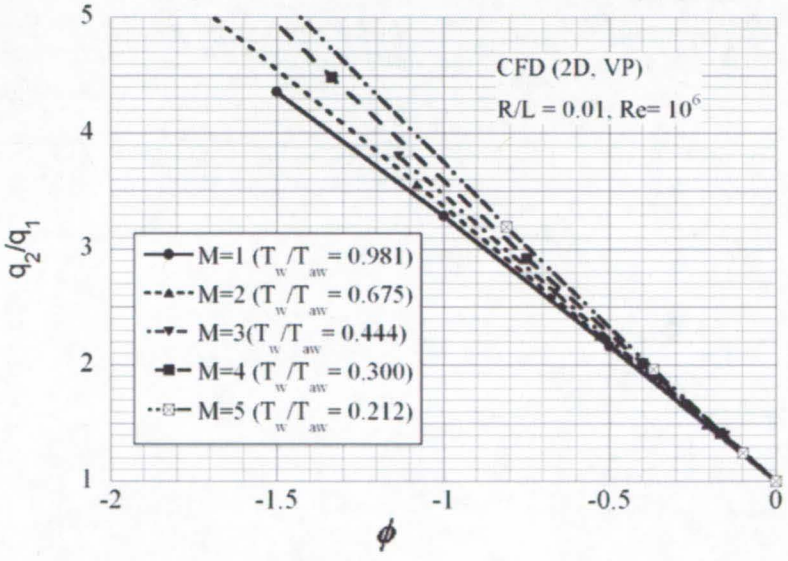

Fig. 8 Variation of heat flux correction factors with Mach number for R/L = 0.01 from 2D CFD with variable properties.